LOWLAND TECHNOLOGY INTERNATIONAL Vol. 10, No. 1, 27-41, June 2008
International Association of Lowland Technology (IALT), ISSN 1344-9656

BEHAVIOUR OF LATERALLY LOADED RIGID PILES IN COHESIVE SOILS BASED ON KINEMATIC APPROACH

V. Padmavathi[1], E. Saibaba Reddy[2] and M. R. Madhav[1]

ABSTRACT: Piles are useful in lowland areas in order to improve the properties of the soil. Several methods are available to predict the ultimate lateral resistance of a rigid pile in clays. The existing solutions for ultimate lateral resistance of rigid piles in clays are either semi-empirical in nature or based on approximate analysis with several simplifications. In most of these methods, the behaviour of soil is assumed as plastic throughout the analysis including at the point of rotation. Even though the ultimate lateral loads predicted by these methods are somewhat comparable with the measured values, the lateral pressure distributions are not consistent. A new approach based on kinematics and non-linear subgrade (hyperbolic) response has been developed to study the load-displacement response of a single rigid pile with free-head in cohesive soils. The predicted ultimate lateral capacities of the piles as well as the lateral soil pressure distributions along the pile length compare well with the results of available theories and experimental test results.

Keywords: Lateral load, rigid pile, non-linear subgrade response, cohesive soil, kinematics, ultimate load

INTRODUCTION

Design of foundations subjected to large lateral forces caused by wind, wave action, earthquake and lateral earth pressures is a challenging task especially if founded in soft ground usually prevalent in lowland regions of the world. Structures such as transmission line towers, bridges, tall buildings, which are usually founded on piles, must be designed to support both axial and lateral loads and moments. The lateral resistance of piles is governed by several factors, the most important being the ratio of the structural stiffness of the pile to the soil stiffness. The relative stiffness of the foundation element with respect to the soil controls the mode of failure and the manner in which the pile behaves under an applied lateral load.

Extensive theoretical and experimental studies have been carried out by several investigators on laterally loaded piles to determine their ultimate lateral loads and displacements, under working loads. Matlock and Reese (1960) define the relative rigidity of a laterally loaded pile in terms of the ratio of the flexural stiffness of the pile, EI, and the coefficient of lateral subgrade reaction, k_s. Their method is applicable only if the deflection of piles is within the range of linear deformation of the soil. Vesic (1961), Davisson and Gill (1963), Broms (1964), Banerjee and Davies (1978) and Poulos and Davis (1980) define and utilize a stiffness ratio, K_r, as

$$K_r = E_p I_p / E_s L^4 \quad (1)$$

where E_s - is the deformation modulus of the soil, E_p - the modulus of elasticity of the pile material, I_p – the moment of inertia of pile cross-section and L - the length of the pile. The pile usually behaves as a rigid one for K_r values greater than 10^{-2}.

Kasch et al. (1977) have proposed that embedded length to diameter ratio, L/d, of the pile also be used to assess the flexural behaviour of the pile and concluded that in order to ensure rigid behaviour, the L/d ratio should not exceed about 6. However, under some conditions, a foundation can have L/d ratio as high as 10 and still behave as a rigid one, but, for flexible behaviour L/d should be in excess of 20. Based on the studies of Meyerhof et al. (1981, 1985), the pile behaviour is rigid even though L/d is as high as 16. From the above studies, it is felt that assessing the rigid behaviour of the pile through relative stiffness factor, K_r, would be a better option. Failure of rigid or short shafts takes place when the lateral earth pressure resulting from lateral loading attains the limiting lateral resistance of the supporting soil along the full length of the member. The rigid pile is assumed to be infinitely stiff and the only motion allowed is pure rotation of the shaft as a rigid body about

[1] Dept. of Civil Engineering, JNTU College of Engg., Hyderabad, Andhra Pradesh, INDIA
[2] Dept. of Civil Engineering, JNT University, Kukatpally, Hyderabad, Andhra Pradesh, INDIA
Note: Discussion on this paper is open until December 31, 2008

some point on the axis of the shaft. For rigid body motion, the rotation of the shaft and the displacement at the ground line define the deformed position of the pile. Broms (1964) assumed that the ultimate soil resistance is developed all along the length for a rigid pile, whereas for a flexible pile, the ultimate load-carrying capacity is arrived at also from the consideration of failure of the pile itself because of the development of a plastic hinge in the pile. Barber (1953) evaluated lateral deflections of piles at working loads using the concept of subgrade reaction considering the boundary conditions both at the ground surface and at the tip of each individual pile. The behaviour at working loads was analysed by assuming the laterally loaded pile to behave as an elastic member and the supporting soil as a linearly deforming material.

Extensive theoretical and experimental studies on laterally loaded piles in clays have been carried out by Broms (1964), Druery and Ferguson (1969), Bhushan et al. (1979), Briaud et al. (1983), Randolph and Houlsby (1984), Meyerhof et al. (1985), Lai and Booker (1989), Narasimha Rao and Mallikarjuna Rao (1995), Prasad (1997), McDonald (1999), etc. All the theoretical studies for the estimation of the ultimate capacity of a single pile were based on mobilization of ultimate lateral soil resistance over the full length of the pile for plastic conditions. In the present study, the kinematics of pile movement is coupled with non-linear response of the in-situ soil to predict the response of the pile under lateral load.

BEHAVIOUR OF PILE AND SOIL

The considered failure mechanisms and the resulting distributions of mobilized soil reactions at failure along a laterally loaded free-head pile driven into a cohesive soil for the estimation of its ultimate lateral capacity is shown in Fig. 1. Soil located in front of the loaded pile close to the ground surface may heave upwards, i.e. the direction of least resistance, while the soil located at some depth below the ground surface moves laterally around the pile. The pile may get separated from the soil on its rear down to a certain depth below the ground surface. The ultimate soil resistance for piles in purely cohesive soils increases with depth from $2c_u$ at the ground surface to 8 to 12 times c_u at a depth of about three pile diameters below the surface (Poulos 1980).

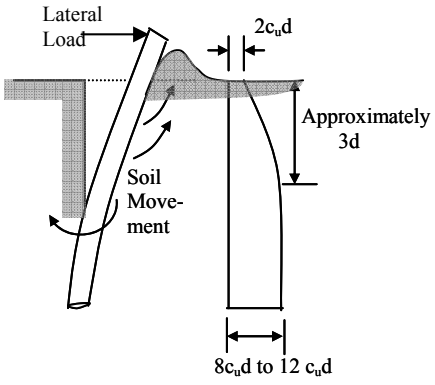

Fig. 1 Pile soil behaviour and postulated distribution of ultimate soil resistance

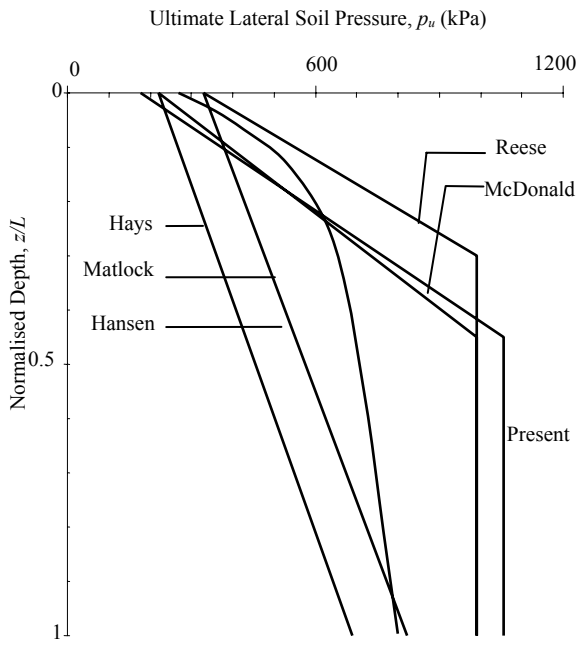

Fig. 2 Ultimate Soil Reaction for Piles in Cohesive Soil by Different Approaches for Typical Values c_u=110 kPa, γ= 20 kN/m^3, d=0.9 m and L=6.0 m

ULTIMATE SOIL REACTION

Hansen (1961), Matlock and Reese (1960), Reese (1958), Broms (1964), Hays et al. (1974), McDonald (1999) have proposed different approaches to compute the ultimate soil reaction, p_u, with depth. The proposed relationships are:

1. Hansen: $p_u = K_c.c_u d$ (2)
2. Matlock: $p_u = [3+(\gamma z/c_u)+(0.5z/d)]c_u d$ (3)
3. Reese: $p_u = [3+(\gamma z/c_u)+(2.83z/d)]c_u d$ (4)
4. Hays: $p_u = 2\eta\, c_u d + \alpha z$ (5)
5. McDonald: $p_u = 2c_u d + (2.33z/d)\, c_u d$ (6)

in which p_u – is the ultimate soil reaction, γ – unit weight of the overburden material, z - depth below the ground line, c_u - undrained shear strength of the soil, d - pile diameter, K_c - earth pressure coefficient given by

Hansen, η - soil strength reduction factor and α - slope of a reaction curve.

All these theories recommend a limiting value for the soil reaction at a critical depth below the ground surface. The limiting value for the soil resistance according to Matlock, Reese, Hays et al. and McDonald theories is $9c_u d$ while Hansen defines the limit as $8.14c_u d$. The ultimate soil reaction by different methods is shown in Fig. 2 for typical values of c_u = 110 kPa, γ = 20 kN/m^3, d = 0.9 m and L = 6.0 m.

LATERAL PRESSURE DISTRIBUTION ACROSS THE DIAMETER

In most of the published theories, it is assumed that the soil pressure acts uniformly along the projected width of the pile, which, for a circular pile, is its diameter as shown in Fig. 3(a). However, the lateral pressure varies along the pile surface (Bierschwale 1981) having a maximum in the direction of applied lateral load and decreasing significantly beyond an angle of 30° as shown in Fig. 3(b). Similar type of behaviour was reported by Reese and Cox (1969), Randolph and Houlsby (1984), and Lai and Booker (1989) from the analysis of piles subjected to lateral loads.

Prasad and Chari (1999) proposed that the lateral pressure is maximum at the centre, that is, in the direction of the load, but decreases to almost zero at the two edges. An average pressure of 0.8 times the maximum pressure is recommended to account for the non-uniform pressure distribution along the pile periphery. Briaud et al. (1983) and Zhang et al. (2005) also proposed shape factors of 0.8 for circular and 1.0 for square and rectangular shapes to account for the non-uniform distribution of soil pressure in front of the pile.

LATERAL PRESSURE DISTRIBUTION ALONG THE LENGTH OF THE PILE

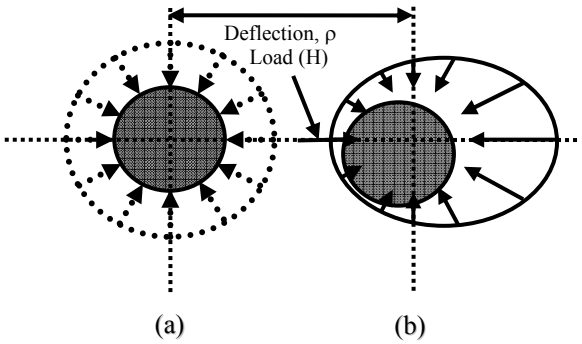

Fig. 3 Pressure distribution around the pile (a) before and (b) after application of lateral load

For a free head rigid pile in a cohesive soil Broms (1964) suggested a simplified distribution of soil resistance as being zero from the ground surface to a depth of 1.5 times the pile diameter and a constant value of $9c_u$ below this depth as shown in Fig. 4(a). This is sometimes mistakenly interpreted to account for possible shrinkage away from the pile in the near surface zone. For large diameter bored pile foundations, the assumption of zero soil resistance to a depth of $1.5d$ is conservative. This is especially true for short piles having slenderness ratio, L/d, less than 5 (McDonald 1999).

A more rigorous distribution (Poulos 1971), in which the soil resistance is equal to the unconfined compressive strength ($2c_u$) of the soil at the surface increasing to 4.5 times of this value at a depth equal to three times the pile diameter, requires the solution of a cubic equation. McDonald (1999) presented solutions for short rigid piles in clay using the soil pressure distribution (Fig. 4b) of $2c_u$ at GL and $9c_u$ as the limiting pressure at a depth of $3d$ from GL (Poulos 1971). The results from McDonald (1999) indicate that Broms estimates of the ultimate pile resistance values are conservative for smaller L/d values. In this paper, the soil pressure distribution along the pile is non-linear as shown in the Fig. 4(c).

Meyerhof et al. (1984 and 1985) and Sastry and Meyerhof (1986) present results from experimental studies for the lateral load capacity of short rigid piles in sand and clay. Soil resistance distributions along the pile length were measured on laterally loaded model piles instrumented with pressure transducers.

STATEMENT OF THE PROBLEM

A pile is subjected usually to a combination of axial and lateral loads and moments. In the present paper, free head rigid pile installed in a cohesive soil subjected to

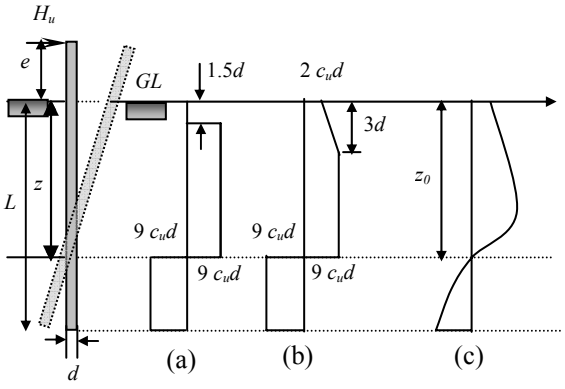

Fig. 4 Pressure distributions along the pile under ultimate lateral load for (a) Broms (1964) and (b) McDonald (1999), Poulos (1971) and at large displacements (c) Present approach

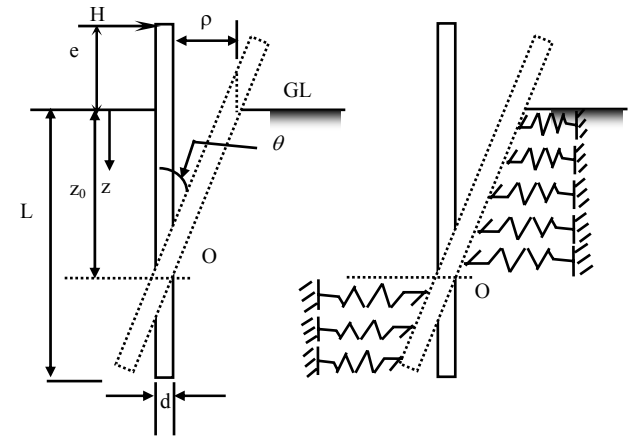

(a) (b)

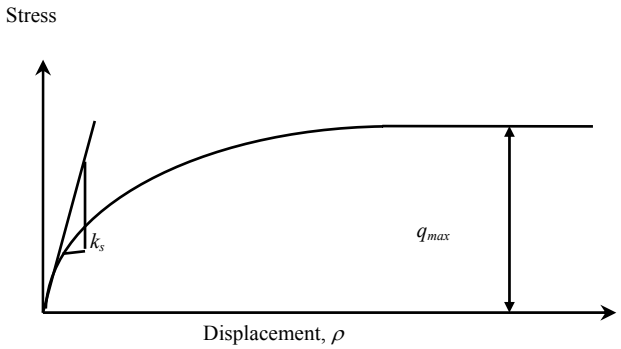

(c)

Fig. 5 (a) Definition sketch (b) Winklers' model (c) Non-linear response of the soil

lateral load only is considered. The pile of length, L, and diameter, d, is acted upon (Fig. 5a) by a lateral force, H, at an eccentricity, e, creating a moment, M (=$e.H$). The pile is unrestrained and rotates through an angle, θ, about a point 'O' at depth, z_0, from the ground surface. The response of the soil is represented by Winkler using a set of springs (Fig. 5b) with modulus of subgrade reaction, k_s, and ultimate lateral soil pressure, q_{max}. The displacement thus varies linearly with depth. The lateral stress, q, is related to the lateral displacement by the hyperbolic relation (Fig. 5c)

$$q = \frac{k_s \rho_z}{1 + \frac{k_s \rho_z}{q_{max}}} \tag{7}$$

where ρ_z is the displacement of the pile at depth, z, from ground surface. k_s is assumed constant with depth and q_{max} varies from $2c_u$ at GL and to a limiting pressure of $12c_u$ (Poulos 1980) at a depth 3 times the diameter.

The force equilibrium equation is

$$H = \int_0^{z_0} q_t d\, dz - \int_{z_0}^{L} q_b d\, dz \tag{8}$$

$$\text{or } H = \int_0^{3d} q_{t1} d\, dz + \int_{3d}^{z_0} q_{t2} d\, dz - \int_{z_0}^{L} q_b d\, dz \tag{9}$$

$$\text{or } H = \int_0^{3d} \frac{k_s \rho_z}{1 + \frac{k_s \rho_z}{q_{max}}} d\, dz + \int_{3d}^{z_0} \frac{k_s \rho_z}{1 + \frac{k_s \rho_z}{q_{max}}} d\, dz$$

$$- \int_{z_0}^{L} \frac{k_s \bar{\rho}_z}{1 + \frac{k_s \bar{\rho}_z}{q_{max}}} d\, dz \tag{10}$$

where q_t and q_b are the lateral stresses above and below the point of rotation respectively with q_{t1} and q_{t2} being the lateral stress for depths from GL to $3d$ and from $3d$ to the point of rotation respectively.

The moment equilibrium equation is

$$M = H.e = -\int_0^{3d} q_{t1} z\, d\, dz - \int_{3d}^{z_0} q_{t2}\, z\, d\, dz + \int_{z_0}^{L} q_b z\, d\, dz \tag{11}$$

$$\Rightarrow M = H.e = -\int_0^{3d} \frac{k_s d\, z\, (z_0 - z)\tan\theta}{1 + \frac{k_s (z_0 - z)\tan\theta}{(2 + 10z/3d)c_u}} dz - \int_{3d}^{z_0} \frac{k_s d\, z\, (z_0 - z)\tan\theta}{1 + \frac{k_s (z_0 - z)\tan\theta}{12c_u}} dz + \int_{z_0}^{L} \frac{k_s d\, z\, (z - z_0)\tan\theta}{1 + \frac{k_s (z - z_0)\tan\theta}{12c_u}} dz \tag{12}$$

where $\rho_z = (z_0 - z)\tan\theta$ and $\bar{\rho}_z = (z - z_0)\tan\theta$ are the displacements at depth, z, above and below the point of rotation, O, respectively.

Normalizing equations 10 & 12 and simplifying

$$H^* = \frac{H}{k_s d L^2} = \int_0^{3\bar{d}} \frac{(\bar{z}_0 - \bar{z})\tan\theta}{1 + \frac{\mu(\bar{z}_0 - \bar{z})\tan\theta}{2 + 10\bar{z}/3\bar{d}}} d\bar{z} + \int_{3\bar{d}}^{\bar{z}_0} \frac{(\bar{z}_0 - \bar{z})\tan\theta}{1 + \frac{\mu(\bar{z}_0 - \bar{z})\tan\theta}{12}} d\bar{z} - \int_{\bar{z}_0}^{1} \frac{(\bar{z} - \bar{z}_0)\tan\theta}{1 + \frac{\mu(\bar{z} - \bar{z}_0)\tan\theta}{12}} d\bar{z} \tag{13}$$

$$M^* = \frac{M}{k_s d L^3} = H^*.e/L = -\int_0^{3\bar{d}} \frac{\bar{z}(\bar{z}_0 - \bar{z})\tan\theta}{1+\frac{\mu(\bar{z}_0-\bar{z})\tan\theta}{2+10\bar{z}/3\bar{d}}} d\bar{z} - \int_{3\bar{d}}^{\bar{z}_0} \frac{\bar{z}(\bar{z}_0 - \bar{z})\tan\theta}{1+\frac{\mu(\bar{z}_0-\bar{z})\tan\theta}{12}} d\bar{z} + \int_{\bar{z}_0}^{1} \frac{\bar{z}(\bar{z} - \bar{z}_0)\tan\theta}{1+\frac{\mu(\bar{z}-\bar{z}_0)\tan\theta}{12}} d\bar{z} \quad (14)$$

where $\bar{z} = z/L$ - the normalized depth, $\bar{z}_0 = z_0/L$ - normalized depth of point of rotation $d = d/L$ – normalized diameter and $H^* = H/k_s d L^2$ - normalized load. The relative stiffness factor for the soil, μ, is defined as

$$\mu = \frac{k_s L}{c_u} \quad (15)$$

Ideally, the depth of rotation, z_0, and the angle of rotation, θ, are to be estimated for a given lateral force, H, and moment, M. It would be an iterative process and very tedious. Alternately, for given values of μ, θ, L/d and e/d, values $\bar{z}_0$ and H^* can be obtained directly by solving Eqs. 13 and 14. Knowing $\bar{z}_0$ and θ, the normalized displacement at ground level, $\rho^* = \bar{z}_0 \tan\theta$, is calculated corresponding to the normalized applied load, H^* (Eq. 13).

RESULTS AND DISCUSSION

The variation of H^* with ρ^*, based on the proposed model, is presented in Fig. 6, for μ values ranging from 0 (infinitely strong soil or linear response) to 10000 (very soft soil) and for no moment at ground level, i.e. $e/d = 0$ and $L/d = 4$. The normalized lateral load, H^*, increases as expected with normalized displacement, ρ^*. The load versus displacement curve is linear for $\mu = 0$, i.e.

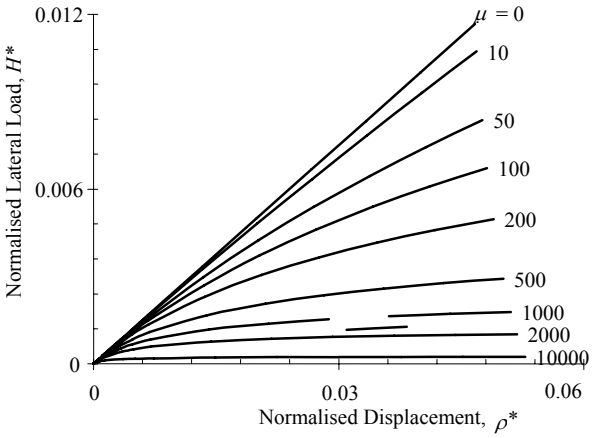

Fig. 6 Normalized load, H^*, vs displacement, ρ^*, at GL for $e/d = 0$ and $L/d = 4$

infinitely large value of undrained shear strength, c_u, or linear response of the ground. Increasing values of μ correspond to decreasing values of the undrained shear strength of the soil and hence the response curves become non-linear, the normalized ultimate lateral load of the pile decreases and is attained at very large displacements. Very low ultimate capacities of the pile

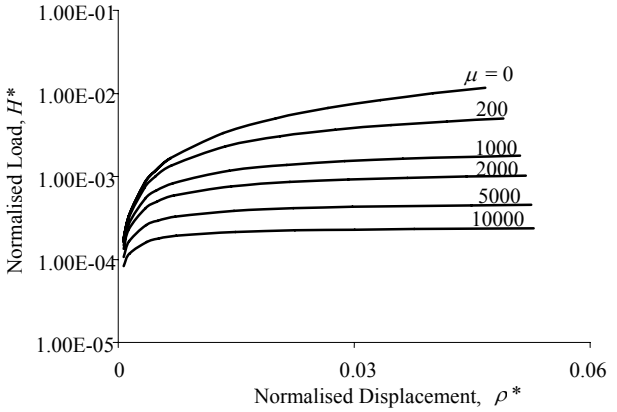

Fig. 7 Normalized load, H^*, vs displacement, ρ^* for e/d=0 and $L/d = 4$

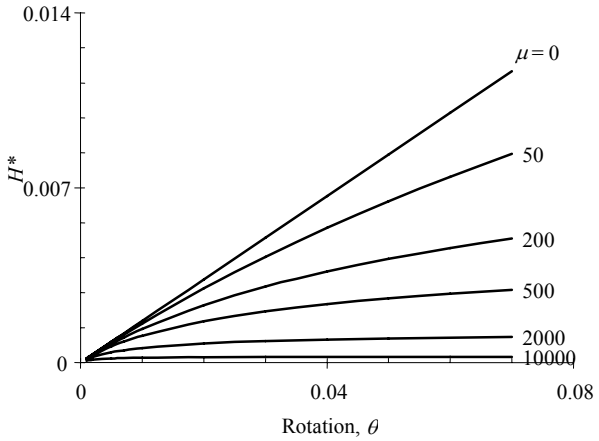

Fig. 8 Normalized load, H^* vs rotation, θ for $e/d = 0$ and $L/d = 4$

are attained at relatively smaller lateral displacements only for very large values of μ, i.e. extremely small ultimate soil resistances.

Ultimate lateral resistance of the pile cannot be obtained precisely from many of the curves in Fig. 6. The normalized ultimate lateral load can easily be estimated from the plot for μ values in the range 1000 to 10000. On the other hand, it is difficult to estimate the ultimate load on the pile for μ values between 0 and 1000, since the loads are predicted upto normalized displacements of 0.06. The variation of normalized

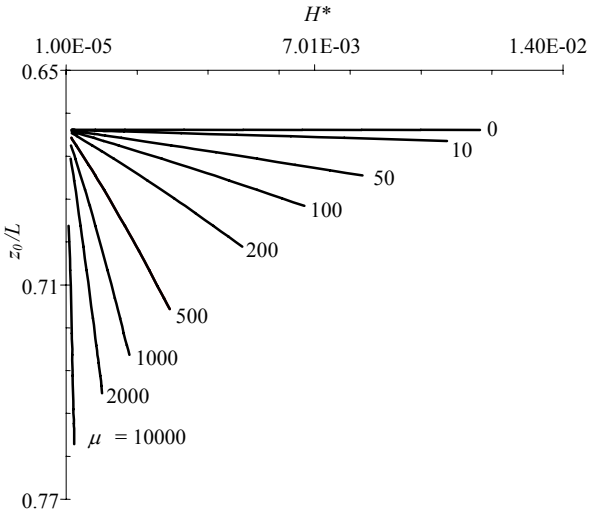

Fig. 9 Movement of normalized depth to point of rotation, z_0/L with respect to H^* and μ for e=0 and $L/d = 4$

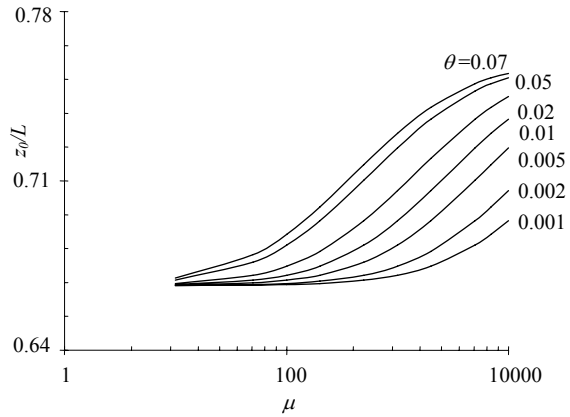

Fig. 10 Normalized depth to point of rotation with μ and rotation, θ for $e/d = 0$ and $L/d = 4$

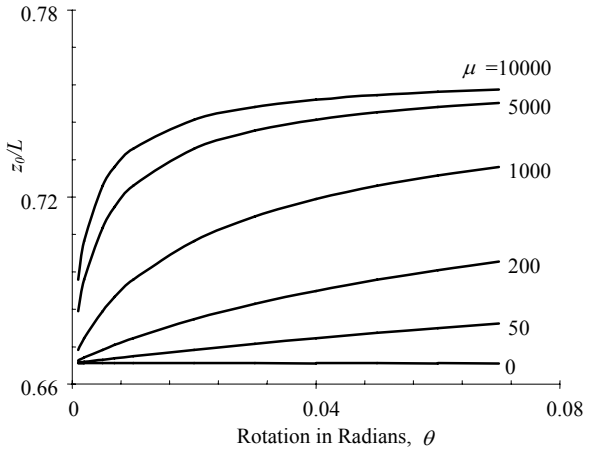

Fig. 11 Normalized depth to point of rotation, z_0/L with μ and rotation, θ, for $e/d = 0$ and $L/d = 4$

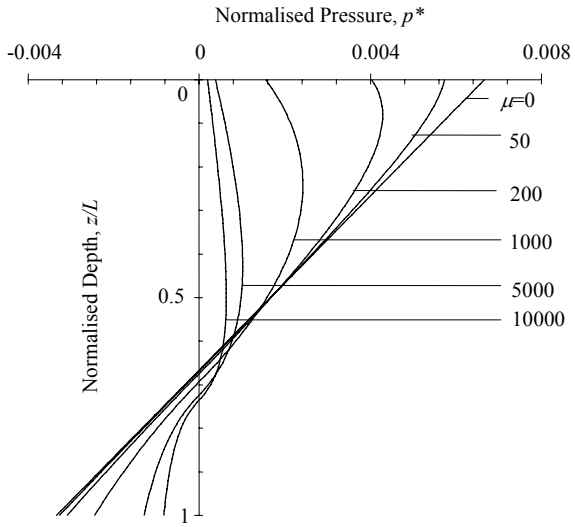

Fig. 12 Normalized pressure distribution with depth, z/L, for $\theta = 0.01$ for e/d = 0 and $L/d = 4$ - effect of μ

displacement, ρ^* with H^* on log scale (Fig. 7) presents the data in a somewhat better manner. The curves presented in Fig. 7 are extrapolated to predict the ultimate lateral loads for values of $\mu < 1000$.

The variation of H^* with rotation, θ, is depicted in Fig. 8 for $e/d = 0$ and $L/d = 4$. The variations of the normalized load with θ for different values of μ are very similar to those depicted in Fig. 6 with respect to displacements since displacement at the top is linearly proportional to rotation. For small μ values (μ <10), the variation H^* with θ is almost linear. The ultimate value of H^* is attained at smaller values of rotation for higher values of μ. Similar trend is observed for other values of e/d and L/d.

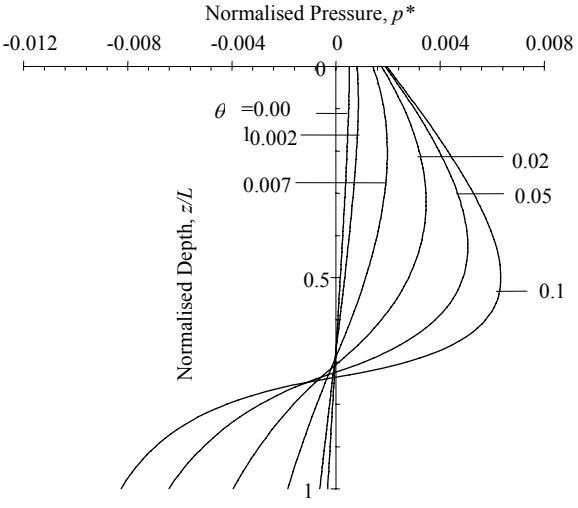

Fig. 13 Normalized pressure distribution with depth, z/L, for $\mu = 1000$, $e/d = 0$, $L/d = 4$ – effect of θ

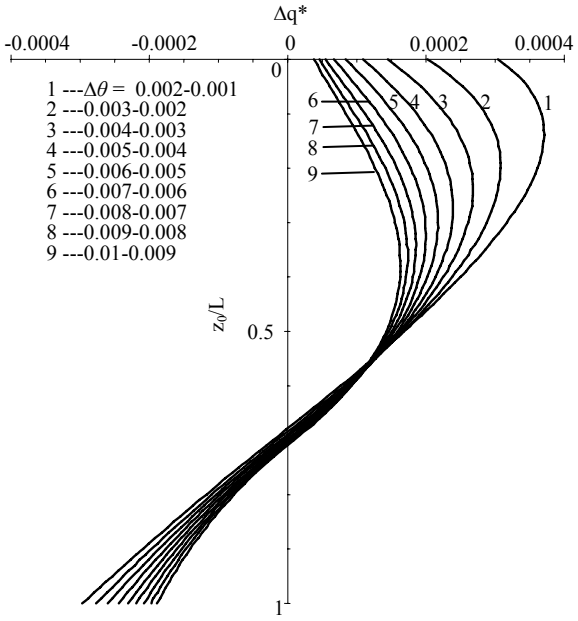

Fig. 14 Incremental of normalised pressure distributions μ = 1000, *e/d*=0, and *L/d* = 4 for θ = 0.001- 0.01

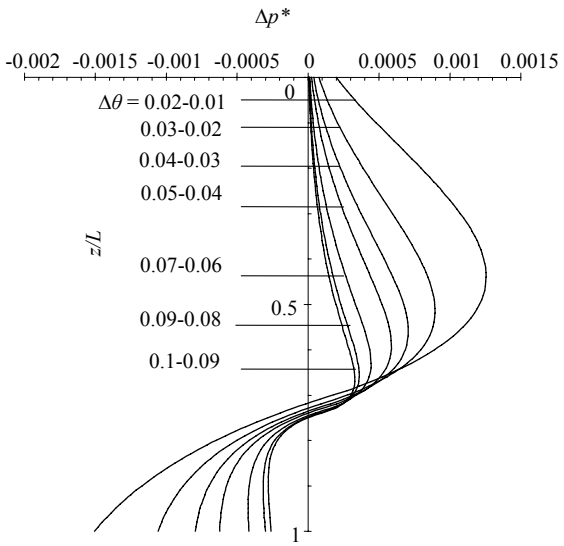

Fig. 15 Incremental of normalized pressure distributions for μ = 1000, *e/d* = 0 and *L/d* = 4 for θ = 0.01 - 0.1

The variation of the depth to the point of rotation with normalized force, H^*, for *e/d* = 0 and *L/d* = 4 is linear and most interesting (Fig. 9). For smaller values of μ (μ <50) the depth to the point of rotation is nearly constant (=0.667) with increase in the normalized load, H^* .However, the depth to the point of rotation increases with H^*, for μ >50, the rate increasing with μ. For μ value of 1000, the normalized depth to the point of rotation increases from 0.67 to about 0.73 as the ultimate capacity of the pile is attained.

Figure 10 shows the variation of normalized depth to the point of rotation, z_0/L, with rotation, θ and μ for *e/d* = 0 and *L/d* = 4. As mentioned earlier, the depth to the point of rotation is almost constant at a value of 0.667 for smaller values of μ. The rate of increase of the normalized depth to the point of rotation with μ increases with increasing values of θ. Also, the rate of increase of the depth to the point of rotation with θ increases with increasing μ and attains asymptotically the final value, e.g. 0.75 for μ =10000, (Fig. 11) for *e/d* = 0 and *L/d* = 4.

The variation of the normalized pressure, *p**, with normalized depth, *z/L*, at a rotation of 0.01 radians and *L/d* = 4 and *e/d* = 0 is shown in Fig. 12 for different values of μ. The pressure distribution is almost linear for small μ values (strong or stiff soils). The point of rotation moves downwards and the normalized pressure distributions become non-linear with increasing μ values. While the normalised pressure distribution is linear and decreases with normalized depth for strong or stiff soils, the normalized pressures increase somewhat with depth in the upper zone before decreasing with depth at lower depths. The point that should be noted is that even at a rotation of 0.01, the fully plastic state is never attained for any of the curves presented and the soil pressures are very small near the point of rotation.

The distributions of normalized pressure, *p**, with respect to normalized depth, *z/L*, with increasing rotation of the pile are depicted in Fig. 13 for *L/d* of 4, μ of 1000 and for zero eccentricity of applied load. For small rotations the pressure distribution with depth is linear as it reflects the linear response of the soil. With increasing rotation of the pile, the normalized pressures increase as also depth to the point of rotation. The pressure distributions with depth reflect the rate at which the ultimate lateral resistance of the soil is attained away from the point of rotation of the pile. The resistance offered by the soil at the surface cannot increase further with θ as it has already reached its limit or the ultimate value of $2c_u$.

The resistance offered by the soil increases with rotation. However, this increase in the normalized soil pressure at any depth, *z/L*, is controlled by two factors, the distance from the point of rotation and the ultimate soil resistance. The increase in displacements with rotation, θ, decrease towards the point of rotation while the ultimate soil resistance increases with depth, at least up to a depth of three times the diameter. As a result of these two effects, the depth to the point of maximum soil resistance increases with θ upto a depth of about 0.52 for θ=0.1. The resistance of the soil developed decreases rapidly to become zero at the point of rotation. The soil resistance once again increases with

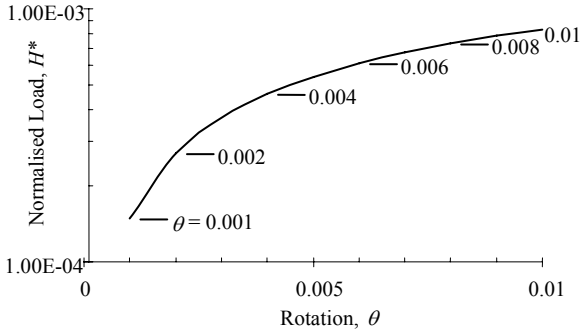

Fig. 16 Normalized load increments with $\theta = 0.001$ - 0.01 for $\mu = 1000$, $e/d = 0$ and $L/d = 4$

depth for points below the point of rotation and tend to attain the ultimate resistance values. The point of rotation moves downwards and the soil pressure in the zone of counter thrust increases rapidly towards the base of the pile. Thus the lateral pressure is less at the top, increases with depth upto the point before becoming zero at the point of rotation as it should be. At depths below the point of rotation, the normalised pressure increases monotonically with depth as the ultimate soil pressures are constant with depth. The pressure distributions obtained are much less than those predicted for the complete or total plastic state assumed by Broms (1964) and McDonald (1999).

To elaborate the above phenomenon, the increments in the values of soil resistances, Δp^*, mobilized at different depths with each increment in rotation, $\Delta\theta$, are presented in Figs. 14 and 15 for increments of 0.001 and 0.01 in rotation for rotations up to 0.01 and 0.1 respectively for $L/d = 4$, $e/L = 0$ and $\mu = 1000$. The increments in soil resistances decrease monotonically with increase in θ. Fig. 16 traces the points along the non-linear load – rotation response curve of the pile for the above case.

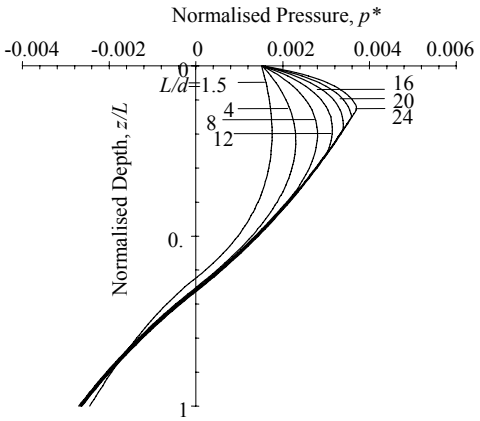

Fig. 17 Normalized pressure, p^* vs z/L – effect of L/d for $\theta = 0.01$, $\mu = 1000$ and $e/d = 1$

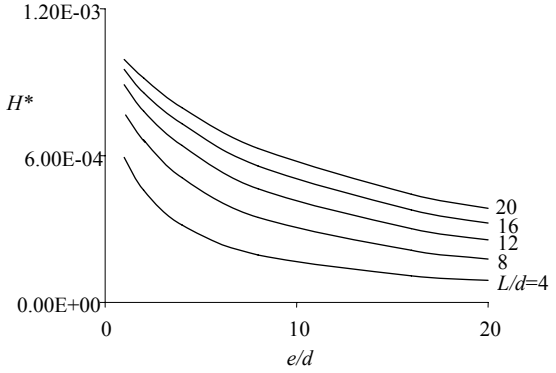

Fig. 18 Normalized load, H^* with e/d – effect of L/d for $\theta = 0.01$ and $\mu = 1000$

Normalized pressure, $p^* = q/k_sL$, versus z/L values are presented (Fig. 17) for different values of L/d and $e/d=1$, $\theta = 0.01$ and $\mu = 1000$. The normalized pressures, $p^* = q/k_sL$, increase with increasing values of L/d. The rate of increase of normalized pressure with depth is high at smaller values of L/d and decreases with increasing values of L/d.

The pressure distribution with depth tends to become asymptotic to a somewhat linear distribution with depth. The normalized pressure distribution varies above the point of rotation, but there is no remarkable variation below the point of rotation for $L/d > 4$.

Figure 18 represents the variation of H^* with normalized eccentricity, e/d, for different L/d ratios of the pile for $\theta = 0.01$. The normalized load, H^*, decreases with increasing eccentricity for all lengths of the piles. The rate of decrease of H^* with e/d is relatively more for e/d less than 10 and much less for e/d greater than 10. The effect of length of the pile on the load carrying capacity is obvious. Longer piles carry larger loads for all eccentricities.

The effect of increasing eccentricities, i.e. increasing values of e/d, reducing the load, H^*, carried by the pile, is explained by the plot in Fig. 19 where in the normal stress, p^*, distribution with depth was plotted for different e/d values, and for $L/d = 4$, $\mu = 1000$, rotation, $\theta = 0.01$. The point of rotation moves up with increasing values of e/d. The areas of the pressure distribution curves above the point of rotation decrease while the areas beneath the point of rotation increase with increasing values of e/d.

Thus the net effect is a decrease in the net horizontal force, H^*, the pile can carry at a given rotation. The rate of change in these areas decreases with increasing e/d with no apparent decrease for e/d greater than 16.

ESTIMATION OF ULTIMATE LATERAL CAPACITY OF THE PILE

For cases where the ultimate lateral capacities of the pile is not clear in the normalized load versus displacement plots, hyperbolic plot suggested by Kondner (1963) is utilized for the estimation of the ultimate lateral capacities. The ratio ρ^* / H^* was plotted against ρ^*, to obtain a straight line. The reciprocal of the slope of the straight line is the normalized ultimate lateral load, H_u^*. The ultimate lateral capacity, H_u, of the pile is then calculated from the expression

$$H_u = H_u^* k_s d L^2 \tag{16}$$

From the studies on hyperbolic response of the soil, the ultimate lateral capacity would be the asymptotic value corresponding to infinite displacement. A reduction factor must be applied in order to obtain a realistic failure load. Based on Jesus (2000), failure load is assumed as 0.75-0.9 times the ultimate load estimated from the hyperbolic plot. In the present paper, the ultimate loads thus estimated from the hyperbolic plots are compared with those predicted by Broms (1964) and McDonalds (1999) theories.

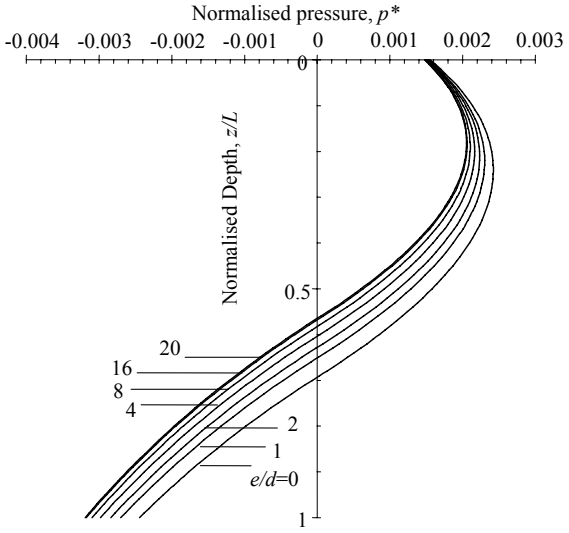

Fig. 19 Normalized pressure, p^* vs z/L – effect of e/d for θ=0.01, μ = 1000 and L/d=4

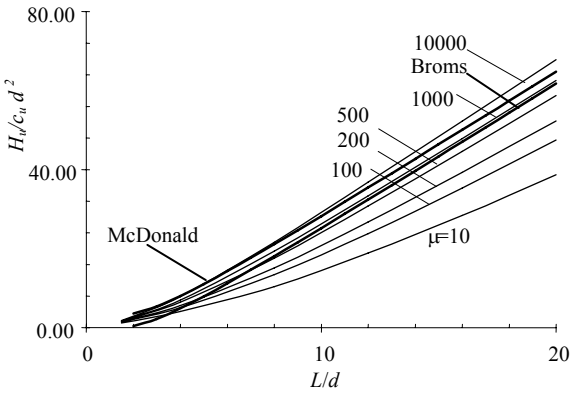

Fig. 20 Variations of ultimate lateral loads with L/d and μ and comparisons with Broms and McDonald approaches for e/d = 0

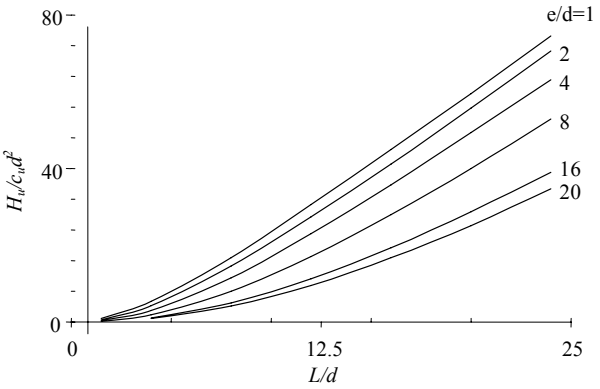

Fig. 21 Ultimate lateral load with L/d – effect of e/d

COMPARISON WITH EXISTING THEORIES

In the present study, Eq. 16 is rewritten and transformed to get normalised ultimate lateral load ($H_u/c_u d^2$) which is convenient to compare with existing theories.

$$\frac{H_u}{c_u d^2} = \frac{H_u^* k_s d\, L^2}{c_u d^2} = H_u^* \mu\,(L/d) \tag{17}$$

The normalized ultimate lateral load ($H_u/c_u d^2$) is estimated using Eq. 17 for each μ and L/d values. The variation of $H_u/c_u d^2$ with respect to μ and L/d are shown in Fig. 20. Relative stiffness factor, μ increases with decrease in strength of the soil. Hence the, ultimate load normalized with $c_u d^2$ values increase with decrease in strength of the soil. But, the absolute value of ultimate load, H_u is less for soft soils (Fig.6) because of less strength of the soil even though the $H_u/c_u d^2$ is very high. Figure 21 gives the variation of $H_u/c_u d^2$, L/d and e/d for μ=1000. As eccentricity increases the ultimate values decrease.

Broms (1964)

Values of $H_u/c_u d^2$ from Broms (1964) approach and the proposed method for piles with different μ values are presented in Fig. 20. Broms (1964) approach under-predicts the ultimate lateral load capacity of the piles for all values of μ and for L/d values less than 4. For L/d values greater than 4 the prediction from Broms' approach is close to the estimated values for μ =1000.

Broms results over-prediction the ultimate lateral loads for strong and stiff clays and under-predict for soft clays. Broms' analysis is conservative for L/d less than 3. The consideration of full mobilization of soil pressure close to the point of rotation (Fig. 4a) eventhough the displacement there, is zero in addition to that the zero soil pressure upto $1.5d$ from ground surface are responsible for these differences in the prediction of ultimate lateral resistance of the pile.

McDonald (1999)

McDonald's theory is based on the ultimate soil pressure distribution shown in Fig. 4(b). Values of $H_u/c_u d^2$ from McDonald's (1999) approach are presented and compared with predictions based on the present approach in Fig. 20. The ultimate lateral load values from McDonald (1999) approach lie very close to the predicted values for very soft (μ=10000) soil but for all other soils (μ<10000), the former are considerably larger than the latter values.

Prasad (1997)

Prasad (1997) presented correlations between the results of static cone penetration, pressuremeter and standard penetration test results and relevant soil properties of cohesive soils to develop methods of analyses for preliminary estimates of ultimate lateral resistance and ground line displacements of rigid and flexible piles.

COMPARISON WITH EXPERIMENTAL RESULTS

Estimation of Soil and Pile-Soil Interaction Parameters

The values of modulus of subgrade reaction, k_s, can be obtained from an actual in situ load-displacement curve. In the absence of such data, modulus of subgrade reaction, k_s, can be estimated from the relation, $k_s=f.(c_u/d)$ where the parameter, 'f' is known to vary in the range of (80-320) for clayey soil (Poulos 1980). The four-fold variation could be due to the dependence of 'f' on the L/d ratio of the pile. In the present study, the values of 'f' considered for the test data based on available correlations are shown in Table 1.

The distribution of soil pressure around the cross section of the pile is non-uniform as stated earlier. Hence, reduction factors of 0.8 and 1.0 are considered for circular and square piles respectively, that is:

$$\mu = \frac{k_s L}{0.8\, c_u} \quad \text{for circular piles} \qquad (18)$$

$$\text{and} \quad \mu = \frac{k_s L}{c_u} \quad \text{for square or rectangular piles} \qquad (19)$$

$H_u/c_u d^2$ and thus values H_u are obtained for known values of L/d, μ and e/d values.

Druery and Ferguson (1969) carried out a series of lateral load tests on free-head model brass piles of 6.35 mm diameter in kaolin to obtain load - displacement curves to failure. Load was applied at eccentricities of 19.05, 25.4 and 33.78 mm. The projected ultimate lateral load values are obtained using hyperbolic relationship. Average undrained shear strength of the soil was 38.8 kPa. The predicted ultimate pile capacities are compared with those from Broms' (1964) and McDonald's (1999) approaches in Table 2. The predictions from Broms' approach are on the higher side while those from McDonald's and the present methods are close to the measured values.

Briaud et al. (1983) reported the results of three field tests conducted on drilled shafts of lengths 6, 4.5 and 4.5 m and diameters 0.9, 0.9 and 0.75 m respectively at a site in Texas A & M University. The soil was stiff clay with average undrained shear strength of 95.8 kPa. The L/d ratios varied from 6.67 to 5. For all the three tests the load eccentricity is zero. As the tests were not carried out upto failure the failure loads were estimated using the hyperbolic relationship and compared in Table 3 with the predictions based on Broms', McDonald's and the present theories.

McDonald (1999) presented extrapolated ultimate lateral loads of four piles of diameter 0.45 m, lengths 1.48, 0.93, 1.4 and 1.0 m and load eccentricities 1.5, 1.05, 1.5 and 1.05 m respectively from field tests in a clay having an average undrained shear strength of 60 kPa. The test details and comparisons are presented in Table 3.

Bhushan et al. (1979) presented five field tests on straight piers, with pier No. 2 tested at site A while pier Nos. 4, 6, 7 and 8 tested at site B. The average undrained shear strength for sites A and B were 260 and 228 kPa respectively. Pier No. 2 was 4.58 m long and 1.22 m in diameter. It was tested at an eccentricity of 0.23 m. For Piers No.s 4, 6, 7 and 8, the lengths and diameters were 3.81, 4.73, 2.75 and 4.73 m and 1.22, 1.22, 0.61 and 0.61 m respectively. All these tests were performed with an eccentricity of 0.23 m. Table 4 compares the measured ultimate capacities with Broms (1964), McDonald's (1999), Prasad's (1997) and the present theories.

Bierschwale (1981) presented three field tests in clay with average undrained shear strength of 110 kPa on piles of different lengths and diameters but with an eccentricity of 0.79 m. The comparisons are presented in Table 5.

Table 1 Proposed factor '*f*' for the calculation of $k_s = f.c_u/d$ values from correlations

c_u kN/m^2	20	50	100	150	200	250
f	170	200	270	310	320	330

Based on all the above comparisons (Tables 2 to 5), ultimate lateral loads predicted by Broms (1964) are conservative if *L/d* values are less than 3 and un-conservative for high *L/d* values which are greater than 6. Pile capacities predicted by McDonald (1999) are, in general, in excess of the measured values for all *L/d* values. Capacities predicted by Prasad (1997) are close to the measured values. However, the ultimate values are based on purely empirical relations. The ultimate capacities from the proposed rational method based on actual kinematics and non-linear response of the soil are close to the measured values.

PREDICTION OF LOAD-DISPLACEMENT RESPONSE OF PILES AT WORKING LOADS

Broms (1964), Poulos (1971) or McDonald (1999) presented only ultimate lateral loads. Briaud et al. (1983) reported measured load - displacement under lateral load for the data given in Table 3. The measured load - displacement curves are compared (Fig. 22) with the predictions based on the present method. The load displacement curves compare well with the experimental data. The measured load-displacement curves are shown in Fig. 23 corresponding to shaft I, II and III based on Bierschwale et al. (1981) which are already specified earlier in Table 5. The load displacement curves are somewhat comparable with experimental curves, but do not match closely, may be because of correlated value of k_s from Table-2. Instead of predicting k_s values from c_u, if k_s values are obtained from load-displacement curves of testing piles, then the predicted load-displacement curves are well coincide with the measured values.

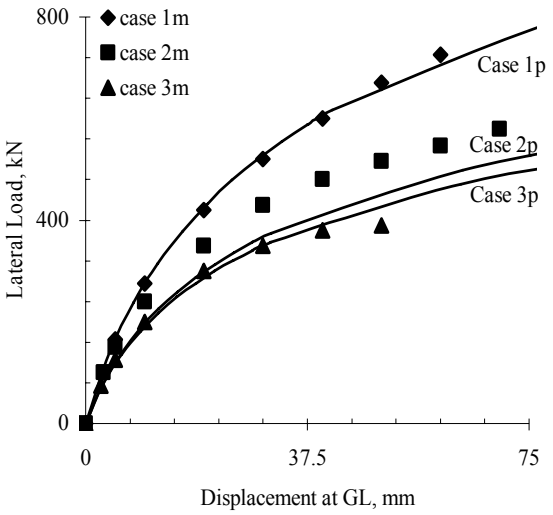

Fig. 22 Comparison of measured vs predicted load deflection curves Briaud et al. (1983) for case 1, case 2 and case 3

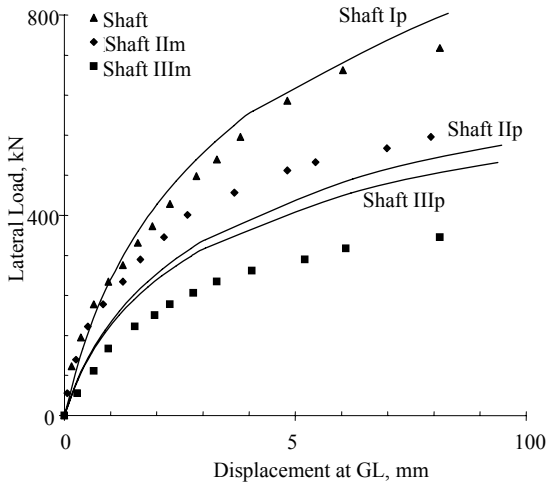

Fig. 23 Comparison of measured vs predicted load deflection curves Bierschwale et al. (1981) for shaft I, shaft II and shaft III

PREDICTION OF SOIL PRESSURE ALONG THE LENGTH OF THE PILE

Bierschwale (1981) also presented lateral pressure distribution of the soil along the shaft for the same

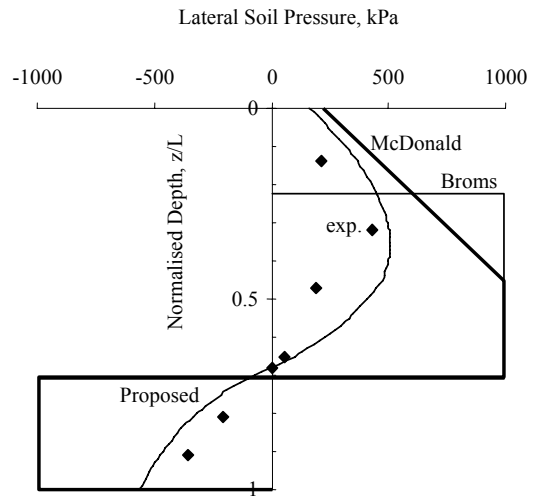

Fig. 24 Lateral soil pressure distribution under ultimate lateral load (752kN) for shaft I Bierschwale et al.(1981)

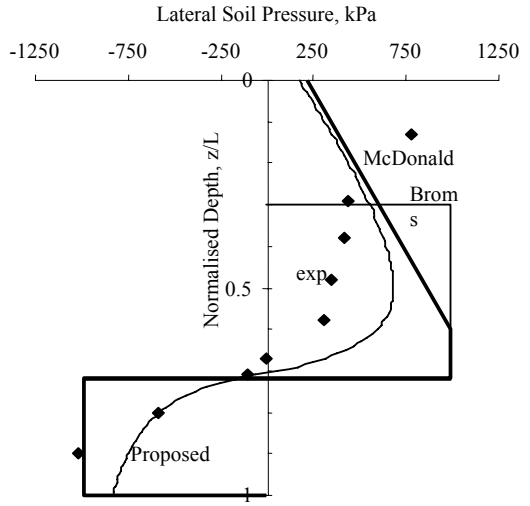

Fig. 25 Lateral soil pressure distribution under ultimate lateral load (667kN) for shaft II Bierschwale et al. (1981)

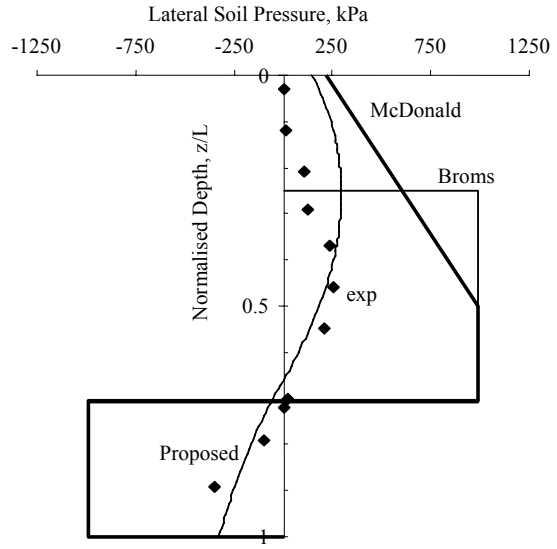

Fig. 26 Lateral soil pressure distribution under ultimate lateral load (400kN) for shaft III (Bierschwale et al. 1981)

parameters as specified in Table 5. These are presented in Figs. 24, 25 and 26 and compared with predictions from Broms, Poulos and McDonald. Even though the ultimate lateral load values are somewhat comparable with measured ones, the distribution of lateral pressures predicted by either Broms or McDonald theories do not match with measured results. The proposed approach predicts both the ultimate pile capacities and the lateral soil resistance distributions with depth, that correlate well with the experimental values. The predicted values are in better agreement with experimental values compared to those from all the other theories.

CONCLUSIONS

The following conclusions are made based on the work presented:

1. A new approach or method based on modulus of subgrade reaction approach is proposed to predict the load-displacement response of laterally loaded free head rigid pile considering nonlinear hyperbolic soil response and kinematics which incorporates the physics of the pile-soil interaction.
2. Broms (1964) approach for predicting the ultimate lateral loads is shown to underpredict the values for L/d<4 and overpredict for L/d >4 for strong or stiff soils corresponding to μ = 1000 in the present theory.
3. Poulos(1971) or McDonald(1999) approach overpredict the ultimate lateral loads for L/d <6. The predictions from their approach for L/d>6 compare well with the values from the present theory for μ = 5000.
4. The present theory, predicts the complete load-displacement response of piles at working loads that fit closely with the experimental values.
5. The distribution of soil resistances along the pile length predicted by the proposed approach compare well with the measured results.
6. An additional correlation is proposed (Table 1) to estimate the values of the modulus of subgrade reaction, k_s.

REFERENCES

Banerjee P.K. and Davies T.G. (1978). The behavior of axially and latterly loaded single piles embedded in non-homogeneous soils. Geotechnique, 28(3): 309-326.

Barber E.S. (1953). Discussion to paper by S. M. Glesser. ASTM., 54: 96-99.

Bhushan K., Haley S.C. and Fong P.T. (1979). Lateral load tests on drilled piers in stiff clays. Journal of the Geotechnical Engineering, ASCE, 105(8): 969-985.

Bierschwale M.W., Coyle H.M. and Bartoskewitz R.E. (1981). Lateral load tests on drilled shafts founded in clay. Presented in Special Session on Drilled Piers and Caissons, ASCE National Convention, St. Louis, Mo.: 98-113.

Briaud J.L, Smith T.P. and Meyer B. (1983). Pressuremetre gives elementary model for laterally loaded piles. International Symposium on In-situ Testing, Paris, 2: 217-221.

Broms B.B. (1964). Lateral resistance of piles in cohesive soils. J. Soil Mech. Found. Div., ASCE. 90(2): 27-63.

Davisson M.T. and Gill H.L. (1963). Laterally loaded piles in a layered soil system. Journal of Soil Mechanics and Foundation Division, ASCE. 89(3): 63-94.

Druery B.M. and Ferguson B.A. (1969). An Experimental Investigation of the Behaviour of Laterally Loaded Piles. B. E. Thesis, Department of Civil Engineering, University of Sydney, Australia.

Hansen J.B. (1961). The ultimate resistance of rigid piles against transversal forces. Bulletin No. 12, Danish Geotechnical Institute, Copenhagen, Denmark: 5–9.

Hays C.O., Davidson J.L., Hagan E.M. and Risitano R.R. (1974). Drilled shaft foundation for highway sign structures. Research Report D647F, Engineering and Industrial Experiment Station, University of Florida, Gainsville, Fla.

Jesús E.G. (2000). Development of an Extended Hyperbolic Model for Concrete-to-Soil Interfaces. Ph.D. Thesis, Department of Civil Engineering, Virginia Polytechnic Institute and State University, Blacksburg, Virginia.

Kasch V. R., Coyle H. M., Bartoskewitz R. E. and Sarver W. G. (1977). Design of drilled shaft to support precast panel retaining walls. Research Report N0. 211.1, Texas Transportation Institute, Texas A&M University, College Station, Tex.

Kondner R. L. (1963). Hyperbolic stress-strain response – cohesive soils. J. Soil Mech. and Found. Div., ASCE. 89(1): 115-143.

Lai J. Y and Booker J. R. (1989). The behaviour of laterally-loaded caissons in purely cohesive soils. Research Report No. R606, The University of Sydney, Australia.

Matlock H. and Reese L.C. (1960). Generalized solutions for laterally loaded piles. J. Soil Mech. Found. Div., ASCE, 86(5): 63-91.

McDonald P. (1999). Laterally loaded pile capacity revisited. Proc. of 8th Australia and New Zealand Conference on Geomechanics, Hobart, 1: 421-427.

Meyerhof G.G., Mathur S.K. and Valsangkar A.J. (1981). Lateral resistance and deflection of rigid wall and piles in layered soils. Can. Geotech. J., 18: 159-170.

Meyerhof G.G. and Sastry V.V.R.N. (1985). Bearing capacity of rigid piles under eccentric and inclined loads. Can. Geotech. J., 22: 267-276.

Meyerhof G.G. and Yalcin A.S. (1984). Pile capacity for eccentric and inclined load in clay. Canadian Geotechnical Journal, 21: 389-396.

Poulos H.G. (1971). Behavior of laterally loaded piles. I: Single piles. J. Soil Mech. and Found. Div., ASCE, 97(5): 711-731.

Poulos H.G. and Davis E.H. (1980). Pile Foundation Analysis and Design. Wiley, New York: 146-147.

Narasimha Rao S. and Mallikarjuna Rao K. (1995). Behaviour of rigid piles in clay under lateral loading. Indian Geotechnical Journal, 25(3): 287-313.

Prasad Y.V.S.N. (1997). Standard penetration tests and pile behaviour under lateral loads in clay. Indian Geotechnical Journal, 27(1): 12-21.

Prasad Y.V.S.N. and Chari T.R. (1999). Lateral capacity of model rigid piles in cohesionless soils. Soils and Found., 39(2): 21-29.

Randolph M.F. and Houlsby G.T. (1984). The limiting pressure on a circularpile loaded laterally in cohesive soil. Geotechnique, 34(4): 613-623.

Reese L.C. (1958). Discussion of soil modulus for laterally loaded piles. by McClelland B. and Focht J.A. Transactions, ASCE, 123: 1071-1074.

Reese L.C. and Cox W.R. (1969). Soil behaviour from analysis of tests on uninstrumented piles under lateral loading. ASTM, STP 444: 160-176.

Sastry V.V.R.N. and Meyerhof G.G. (1986). Lateral soil pressures and displacements of rigid piles in homogeneous soils under eccentric and inclined loads. Can. Geotech. J., 23: 281-286.

Vesic A.B. (1961). Bending of beams resting on isotropic elastic solid. Journal of Engineering Mechanics Division, ASCE, 87(2): 35-53.

Zhang L., Silva F. and Grismala R. (2005). Ultimate lateral resistance to piles in cohesionless soils. J. Geotechnical & Geoenvironmental Engg., ASCE, 131(1): 78-83.

Table 2 Comparisons with Druery and Ferguson (1969) tests

Length of pile in Clay, L (mm)	Diameter of the pile, d (mm)	Load Eccentricity, e (mm)	Average Undrained Cohesion (c_u) kPa.	Estimated Ultimate Load (N)	Ultimate Load by Broms (N)	Ultimate Load by McDonald (N)	Ultimate Load by Proposed Method (N)
146.0	6.35	19.05	38.8	112	96	100	130
139.7	6.35	25.4	38.8	112	86	89	116
132.1	6.35	33.78	38.8	94	74	77	100

Table 3 Comparisons with Briaud et al. (1983) and McDonald (1999) field tests

Length of the pile in Clay, L (m)	Diameter of the pile, d (m)	Load Eccentricity, e (m)	Average Undrained Cohesion (c_u) kPa.	Extrapolated Ultimate Load (kN)	Ultimate Load by Broms (kN)	Ultimate Load by McDonald (kN)	Ultimate Load by Proposed Method (kN)	References
6.00	0.90	0.00	95.80	1111.00	1046.00	1285.00	1250.00	
4.50	0.90	0.00	95.80	769.00	616.00	857.00	769.00	Briaud et al. (1983)
4.50	0.75	0.00	95.80	526.00	604.50	770.70	714.00	
1.48	0.45	1.50	60.00	45.00	15.18	31.40	34.50	
0.93	0.45	1.05	60.00	16.00	2.10	14.60	15.53	McDonald (1999)
1.40	0.45	1.50	60.00	33.00	12.51	28.00	30.70	
1.00	0.45	1.05	60.00	20.00	3.38	16.80	18.10	

Table 4 Comparisons with Bhushan et al. (1979) field tests

Length of the pile in Clay, L (m)	Diameter of the pile, d (m)	Load Eccentricity, e(m)	Average Undrained Cohesion (c_u) kPa.	Ultimate Load at 2° rotation (kN)	Ultimate Load by Broms (kN)	Ultimate Load by McDonald (kN)	Ultimate Load by Prasad (kN)	Ultimate Load by Proposed Method (kN)	References Bhushan et al. (1979)
4.58	1.22	0.23	260.00	1850.00	1513.00	2650.00	2050.00	2500.00	Pier 2, Site A
3.81	1.22	0.23	228.00	1730.00	784.70	1778.60	1450.00	1667.00	Pier 4, Site B
4.73	1.22	0.23	228.00	2050.00	1442.50	2439.30	2370.00	2000.00	Pier 6, Site B
2.75	0.61	0.23	228.00	715.00	488.00	725.00	750.00	667.00	Pier 7, Site B
4.73	0.61	0.23	228.00	1420.00	1368.60	1612.00	1400.00	1667.00	Pier 8, Site B

Table 5 Comparisons with Bierschwale et al. (1981) field tests

Length of the pile in Clay, L (m)	Diameter of the pile, d (m)	Load Eccentricity, e (m)	Average Undrained Cohesion (c_u) kPa.	Extrapolated Ultimate Load (kN)	Ultimate Load by Broms (kN)	Ultimate Load by McDonald (kN)	Ultimate Load by Proposed Method (kN)	Particulars	References
6.100	0.915	0.790	110	1111	1052	1292	1250	Shaft I	Bierschwale et al.(1981)
4.572	0.915	0.790	110	714	591	822	769	Shaft II	
4.572	0.762	0.790	110	476	577	736	714	Shaft III	

LIST OF SYMBOLS

α	=	slope of a reaction curve
c_u	=	undrained cohesion of the soil
d	=	diameter of the pile
e	=	load eccentricity (the distance between point of application of load and ground level)
E_p	=	modulus of elasticity of pile material
E_s	=	average horizontal soil modulus
H	=	lateral load
H^*	=	normalized lateral load
H_u	=	ultimate lateral load
H_u^*	=	normalised ultimate lateral load
η	=	soil strength reduction factor
γ	=	unit weight of the soil
I_p	=	moment of inertia of pile cross section
K_c	=	theoretical earth pressure coefficient given by Hansen
K_r	=	relative stiffness factor
k_s	=	modulus of subgrade reaction
L	=	length of the pile from ground level to toe point
M	=	moment at the ground point
M^*	=	normalized moment at the ground point
μ	=	non dimensional coefficient
p_u	=	lateral resistance per unit length
q_t	=	the lateral stresses above the point of rotation
q_b	=	the lateral stresses below the point of rotation
q_{t1}	=	the lateral stress from GL to 3d depth
q_{t2}	=	the lateral stress from 3d depth to point of rotation
ρ	=	deflection at ground point
ρ^*	=	normalised displacement at ground point
ρ_z	=	deflection above the point of rotation at any depth z from ground point.
$\overline{\rho_z}$	=	deflection below the point of rotation at depth z from ground point.
q_{max}	=	maximum lateral soil pressure
θ	=	angle of rotation in radians
z	=	depth of point under consideration from ground point
z_0	=	depth of point of rotation from the ground point
$\overline{z}_0$	=	normalized depth of point of rotation